Received: 17 February 2023 | Revised: 29 May 2023 | Accepted: 8 June 2023 | Published online: 9 June 2023

RESEARCH ARTICLE

Journal of Computational and Cognitive Engineering
2023, Vol. 2(4) 304–311
DOI: 10.47852/bonviewJCCE3202768

BON VIEW PUBLISHING

Hearing Aid System Response Improvement

Pamraat Parmar[1,*] **and Timothy Sands**[1]

[1]*Sibley School of Mechanical and Aerospace Engineering, Cornell University, USA*

Abstract: This study was conducted to understand the response of hearing aids to different inputs and propose a novel technique to significantly improve performance of hearing aid implants. The motivation behind this study is to represent behavior of hearing aid system with simple input-output relation rather than complicated models. This representation offered a better understanding of the system and inspired an innovation to improve the hearing aid implants. A model of a hearing aid system called cochlear transplants is generated and used to simulate the system response. Using multiple methods, simplified input-output relations are derived. Results from these methods are compared, and conclusions are drawn regarding which method is best for this application. One of the methods used resulted in 69.7 % error measure reduction compared to the benchmark method. This method was later used to produce a simplified model, which was then used as the basis for analysis of different configurations. A qualitative comparison of model was made, and significant improvement of cochlear transplants was achieved.

Keywords: human auditory system, system identification, hearing aid, human ear model, deterministic artificial intelligence, feedforward, Model Predictive Control (MPC)

1. Introduction

Development of human hearing aids started around the 1960s (Loizou, 1998). Loeb (1990), Millar et al. (1984), Parkins and Anderson (1983), and Wilson as well as Dorman (2012) offer an insight into strategies adapted by initial developers. Nobel laureate George von Bekesy deduced similarity in feeling and hearing sensations (von Békésy, 1959), inspired by which he unfolded complex auditory system (von Békésy, 1963). He extended his studies to develop physical models (von Békésy, 1970), which laid the foundation of modern cochlear implants. Hochmair-Desoyer et al. (1983) were among the first notable works in cochlear transplants, which was improved and implemented by Clark et al. (1983). Today, though not everyone, but significantly large types and scales of deafness can be treated by implants (Loizou, 1998). The human auditory system being a complex system, sound processing by the hearing aid is done in different stages, making the models of these implants complicated. A part of this study is to deduce simple input-output relation of these models. This relation is utilized to improve hearing aid performances, which has a potential to radically improve auditory system health management, audio device operations, multimedia experience, and many other applications. One of the more involved applications is analyzing human perception of different sound inputs and their impact on thought processes, thereby aiding medical experts in mental health treatment, or alleviating mental illnesses. The improvement of models is done by incorporating controllers in the general open loop system. Results from different controllers are studied, conclusions are drawn about their performances, and recommendations on their usages are made.

*__Corresponding author:__ Pamraat Parmar, Sibley School of Mechanical and Aerospace Engineering, Cornell University, USA. Email: ppp29@cornell.edu

This article has 6 sections and 3 appendices. Section 2 provides necessary information for the reader to understand the methods and results of the study. This includes basics of human auditory system and hearing aid system explanations. Section 2 also refers to Appendices B and C for in-depth explanation of certain topics readers might not be acquainted with. In Section 3, the study transitions to detailing the methods used and the inputs given. Section 4 presents results from all the methods and their consolidated comparisons. Finally, Section 5 draws conclusions from these results. Readers are advised to refer to Appendix A for the list of acronyms used in the article.

2. Background

For the ease of use of this paper, this section explains the working of human auditory system and explanation of model developed by Loizou (1998).

2.1. Working of human auditory system

Human ear is divided in three regions: (i) Outer Ear, (ii) Middle Ear, and (iii) Inner Ear. The Outer Ear captures the sound, which are referred to as acoustic signals in this article, and directs them to the Middle Ear. The Middle Ear then converts the acoustic signals into mechanical motion, which can be sensed further by the Inner Ear. The function of the Inner Ear is to interpret the motion of Middle Ear and translate it to neuroelectric signals, which are the signals brain can interpret and perceive. The anatomy of the overall ear is given in Figure 1. A detailed explanation of human ear anatomy is given in Appendix B, and the reader is strongly recommended to go through for better clarity of this study.

Figure 1
Anatomy of human ear (image courtesy of "EarQ" (2022))

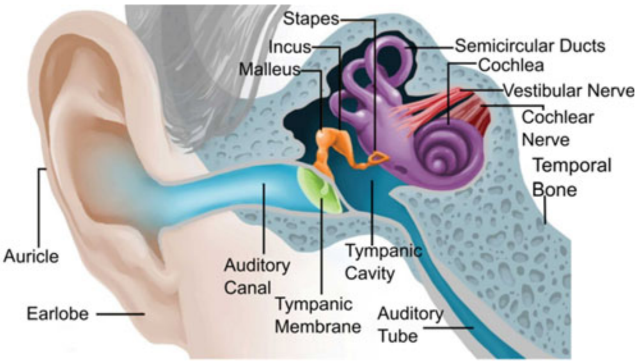

2.2. Human auditory signal processing

The main signal processing unit of the human ear is cochlea. Cochlea manages to derive frequency information with help of a membrane called basilar membrane (BM) (shown in Figure 2).

The BM has linearly varying Young's modulus and different thicknesses (De Paolis et al., 2017), allowing different regions of membrane to vibrate maximally depending on the frequency content of sound. The vibrations in BM cause the fluid in that region to vibrate, which is detected by hair cells of that region. The low-frequency content is detected by the apex of BM, while high-frequency content is detected by the lower regions of BM, as shown in Figure 2. Most observed deafness is due to damage of hair cells, causing person to lose hearing of certain frequencies. This inspires the use of cochlear implants, which stimulate the auditory neurons connected to hair cells directly, helping person to regain hearing.

2.3. Working of cochlear implants

Modern cochlear implants use a system of microphone that picks up a sound, signal processor to convert acoustic signals into electric signals, transmission system that transmits the electrical signal to implants, and implants, which are electrodes, which are inserted in cochlea and stimulate the auditory nerves. Usually, multiple electrodes are planted at different locations shown in Figure 2. The signal processor and transmission systems send only relevant signals to each electrode. Detailed account of cochlear transplant operation is given in Appendix C for interested readers.

2.4. Model of cochlear implants

The model of Cochlear implant is adapted from Loizou (1998). It must be noted that the auditory model developed by Dau et al. (1996a, 1996b, 1997a, 1997b) in 4 sets of paper is the most famous auditory system model. Dau et al. (1996a) and Dau et al. (1996b) quantify the signal processing parameters, and Dau et al. (1997a) and Dau et al. (1997b) model the system and explain the auditory signal modulation techniques. However, a rather simple model is chosen for this study. Moreover, SIMULINK® provides a sample model of implant, which can be used after minor modifications. The block diagram for cochlear transplant is shown in Figure 3.

The input is processed in two steps:

(i) Input signal processing
(ii) Pulse generation

Figure 2
(a) Schematic of basilar membrane and (b) plot of different regions processing different frequency

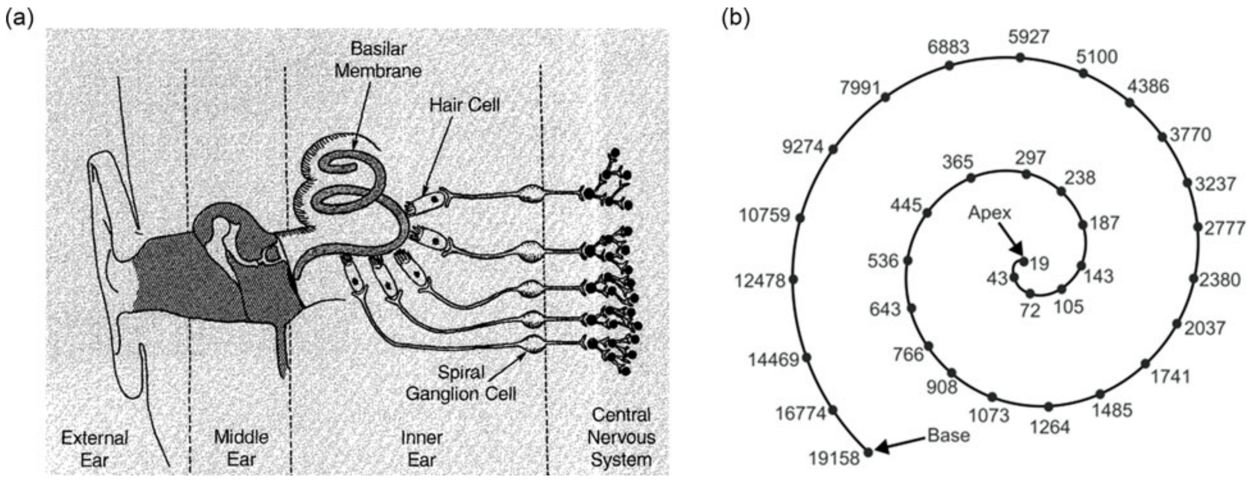

Figure 3
Simulink model of cochlear transplant

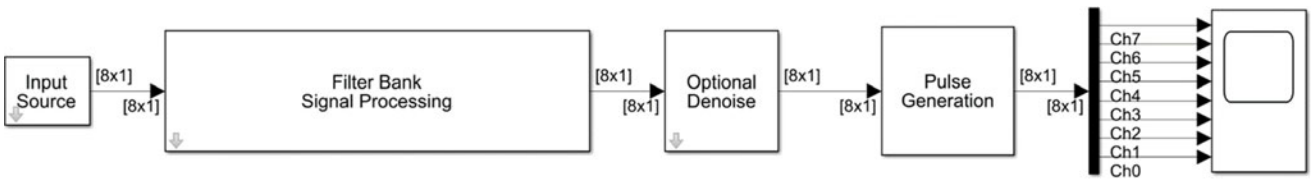

Table 1
Electrode implant frequency band detection range

Channel no.	0	1	2	3	4	5	6	7
Freq. range (Hz)	> 5 k	2.5 k–5 k	1.2 k–2.5 k	600–1200	450–600	300–450	150–300	< 150

For benchmarking, a sweep signal is given as an input. This signal contains frequency components swept from 10 Hz through 10 kHz linearly in 5 s. Eight signals are sampled from sweep signal, as eight electrode system is being modeled here.

The first step is to separate all the frequency content of eight signals into eight frequency bands, corresponding to eight locations on BM. The electrode frequency detection ranges are shown in Table 1.

The first step is done using filter bank signal processing block which contains Cascade Finite Impulse Response (FIR) Bank. The Cascade FIR Bank is not explained here due to lack of relevance; however, reader is recommended to study literature to better understand the model. Before the second step, white noise can be reduced to process a cleaner signal, which is obtained by denoising. In this case, since the test case is clean sweep signal, denoise block is kept off.

The second step is to introduce delayed pulsation. As explained in 2.3, it is better to have signal in form of delayed pulses to avoid inter-electrode interaction. This is the signal sent to electrodes. Electrodes reconstruct and interpret these signals and stimulate the auditory nerves accordingly. The higher the amplitude, the higher the number of auditory nerves are stimulated, thus making the brain perceive the sound louder.

Figure 4 shows the input signal for the first 0.25 seconds, actual signal is frequency sweep from 10 Hz to 10 kHz in 5 seconds. Eighty channels of input data are fed into the model, and each channel is appropriately filtered and pulsated to receive the signal with relevant frequency content. Figure 4 shows the output of 8 channels of the model. In this article, system identification of 600 Hz – 1200 Hz channel is demonstrated and an attempt to improve output characteristics of 10 Hz – 150 Hz channel is presented.

3. Research Methodology

The process of developing mathematical models representing the behavior of a system is called system identification. The identified system is then used to derive system characteristics. The study then proposes methods to improve the system characteristics.

3.1. System identification

The method adapted for system identification of system under consideration is Autoregressive Moving Average (ARMA) (Astrom & Wittenmark, 2013). The ARMA model considers the effect of previous inputs and outputs on the current output and uses it to predict the next output. Let us assume previous p outputs, and q inputs have impact on current output. This is written mathematically in equation (1).

$$y(t) = \alpha_1 y(t-1) + \alpha_2 y(t-2) + \ldots + \alpha_p y(t-p) + \beta_0 u(t) + \beta_1 u(t-1) + \ldots + \beta_q u(t-q) \tag{1}$$

Here, α_i are coefficients of output $y(t)$, and β_i are coefficients of input, $u(t)$. The magnitudes of these coefficients dictate the impact of

Figure 4
(a) Input signal for first 0.25 s, full signal runs for 5 s, (b)–(i) channel outputs of cochlear implant model

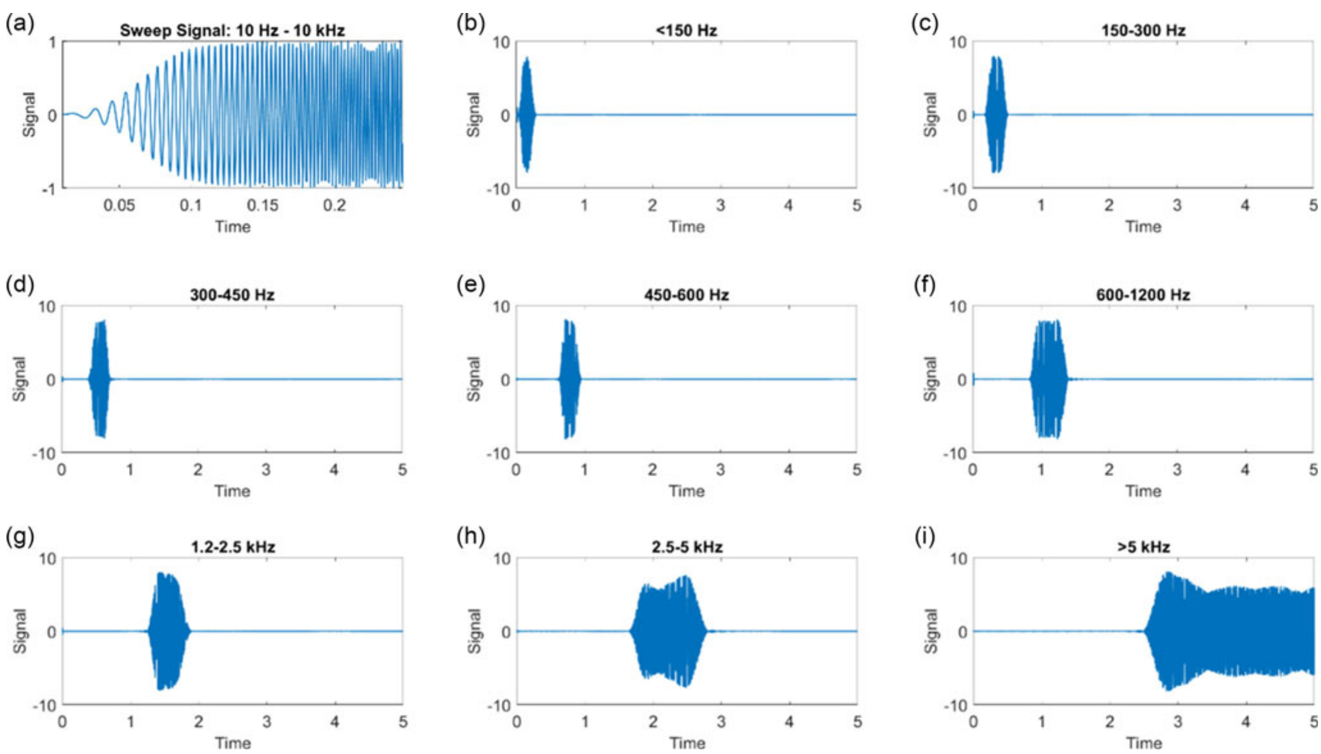

Figure 5
Implant model with MPC controller

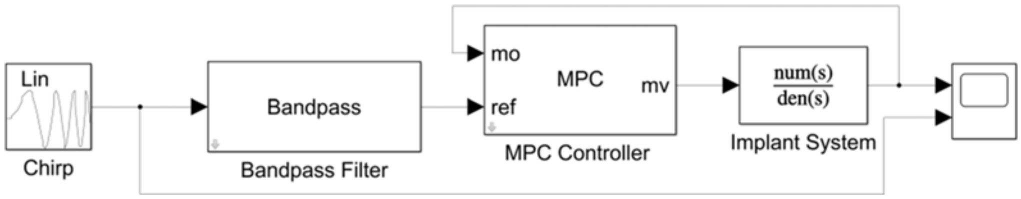

Figure 6
Feedforward/MPC feedback controller

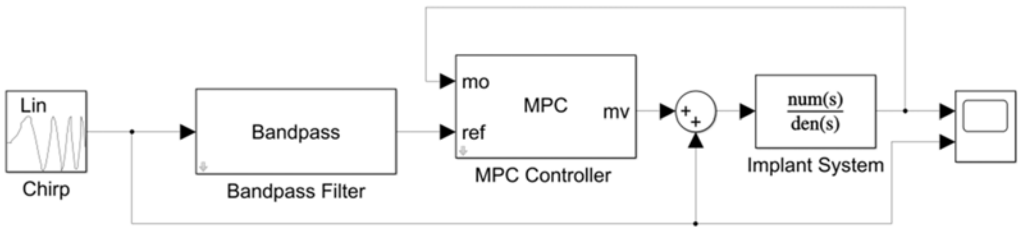

the terms on current output. To write equation (1) concisely, equation (2) is written.

$$y(t) = \mathbf{\Phi}^T(t)\theta \tag{2}$$

Here, ϕ and θ are given by (3).

$$\begin{aligned}\mathbf{\Phi} &= [y(t-1) \quad y(t-2) \quad \ldots \quad y(t-p) \quad u(t) \quad u(t-1) \quad \ldots \quad u(t-q)]^T \\ \theta &= [\alpha_1 \quad \alpha_2 \quad \ldots \quad \alpha_p \quad \beta_0 \quad \beta_1 \quad \ldots \quad \beta_q]^T\end{aligned} \tag{3}$$

When the model of system is not known, θ is unknown. In such cases, we estimate θ by $\hat{\theta}$, and this process of estimation is essentially system identification. $\hat{\theta}$ was estimated using four methods in this study, namely least mean squares, recursive least squares, extended least squares, and extended least squares-posterior residuals.

3.2. Model improvements

After system identification of the model shown in Figure 3, the coefficients are used to predict the transfer function of the cochlear implant system. This transfer function transforms sound signal analyzed by the system to the signals generated by electrodes. The transfer function accounts for dynamics of stapes, oval window, cochlea, and BM. For ease of analysis, the electronic FIR filter circuit with rectifiers and modulators was simply assumed to be a bandpass filter.

Application of a feedback loop in cochlear implant system was attempted. It being a highly nonlinearity system, linear controllers like PID performed poorly for all tried combinations of gains, and PID Tuner app of MATLAB® failed to find feasible solution. Thus, adaptive Model Predictive Controller (MPC) was used in the feedback loop as shown in Figure 5, which showed immense improvement in the response of the system.

A standard feedforward/MPC feedback approach was also attempted as shown in Figure 6. The context of the already commonly defined term "feedforward" used here (differently and more restrictively) is the context of deterministic artificial intelligence (Sands, 2019).

As can be seen in Figures 5 and 6, the input is chirp signal from 2 Hz to 200 Hz, and the bandpass filter has lowpass up to 10 Hz and highpass up to 150 Hz. This filtering model's channel no. 7 (refer Table 1) of actual cochlear implant.

4. Results

The methodologies for system identification and implementation of feedforward/feedback 2DOF system were applied to cochlear implant system, and results achieved are presented below.

4.1. System identification

System identification of 600 Hz – 1200 Hz channel (shown in Figure 4) is conducted. The order of ARMA is 50 both in input and output ($p = 50$, $q = 50$). Order of residuals is chosen as 50 wherever applicable (r=50). Table 2 shows the RMS error values in the system identification and % reduction in value against LMS RMS value. The quality of fit for ELS-PR prediction method, which is the best among all, is shown in Figure 7.

As can be seen in error plots in Figure 7, the error magnitudes of system identification are as high as 60%. The root mean squared (rms) value of error is used to compare the quality of fits. ELS-PR shows 69.7% reduction in rms errors compared to LMS.

Table 2
Table of rms values of error plot for each fitting method

Method	RMS	% Reduction
LMS	0.5215	−NA-
RLS	0.1875	64 %
ELS	0.1872	64.1%
ELS-PR	0.1579	69.7 %

Figure 7
ELS-PR parameter estimation for ARMA

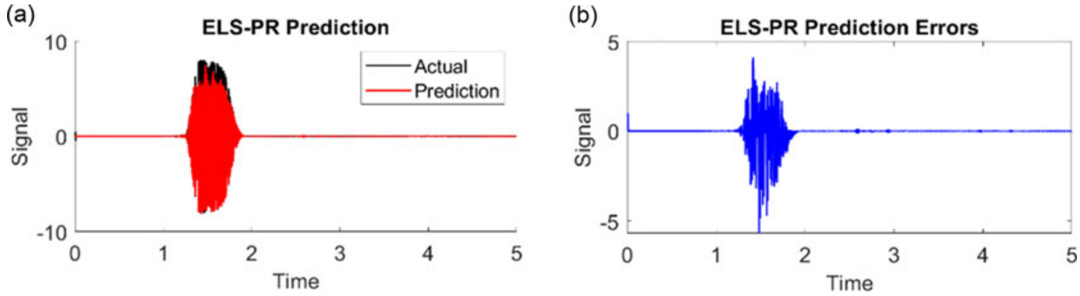

Figure 8
Implant operations with (a) open loop, (b) MPC feedback controller, and (c) feedforward/MPC feedback controller

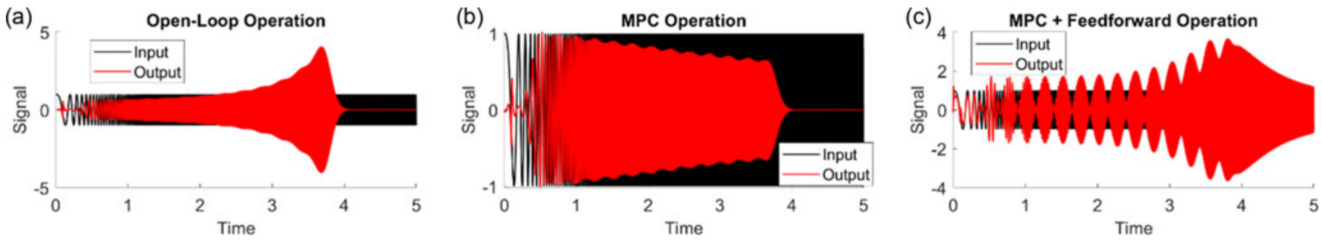

4.2. Model improvement

MPC for both, closed loop with and without feedforward is using control horizon of 2 and prediction horizon of 10. The results of implant operations with different control configurations are shown in Figure 8. The MPC operation without any feedforward component performed the best, as it has provided performance close to the chirp signal. The MPC with feedforward logic surpasses the filter, as the feedforward is taken from the command with all frequency components.

5. Conclusion

The high error magnitudes of system identification (seen in Figure 7) are not due to poor fitting, but because of a delay induced by fitting. In most cases these delays are not observed, however, the high frequency of pulsated data makes the delay apparent in errors. Since the root mean squared (rms) value of error is used to compare the quality of fits, the system identification of for cochlear implant is done using ELS-PR as it produces least rms error.

As can be seen in Figure 8, the MPC controller performs the best among three configurations. The nonlinearity of the plant is so severe that PID controllers cannot be implemented. An interesting point to note in feedforward/MPC feedback controller is that the output in filtered range is consistent. A promising research topic can be using the signal feedforward only in the unfiltered range. At this point, due to high frequency and delay induced by the controller in the circuit, it is not possible to quantify the performance; however, qualitative analysis clearly directs us to use MPC controller in cochlear implants. If implemented, the hearing quality of the patients can be significantly improved.

Conflicts of Interest

The authors declare that they have no conflicts of interest to this work.

References

Astrom, K. J., & Wittenmark, B. (2013). *Adaptive control*. USA: Courier Corporation.

Clark, G. M., Shepherd, R. K., Patrick, J. F., Black, R. C., & Tong, Y. C. (1983). Design and fabrication of the banded electrode array. *Annals of the New York Academy of Sciences*, *405*(1), 191–201. https://doi.org/10.1111/j.1749-6632.1983.tb31632.x

Dau, T., Kollmeier, B., & Kohlrausch, A. (1997a). Modeling auditory processing of amplitude modulation. I. Detection and masking with narrow-band carriers. *The Journal of the Acoustical Society of America*, *102*(5), 2892–2905. https://doi.org/10.1121/1.420344

Dau, T., Kollmeier, B., & Kohlrausch, A. (1997b). Modeling auditory processing of amplitude modulation. II. Spectral and temporal integration. *The Journal of the Acoustical Society of America*, *102*(5), 2906–2919. https://doi.org/10.1121/1.420345

Dau, T., Püschel, D., & Kohlrausch, A. (1996a). A quantitative model of the "effective" signal processing in the auditory system. I. Model structure. *The Journal of the Acoustical Society of America*, *99*(6), 3615–3622. https://doi.org/10.1121/1.414959

Dau, T., Püschel, D., & Kohlrausch, A. (1996b). A quantitative model of the "effective" signal processing in the auditory system. II. Simulations and measurements. *The Journal of the Acoustical Society of America*, *99*(6), 3623–3631. https://doi.org/10.1121/1.414960

De Paolis, A., Watanabe, H., Nelson, J. T., Bikson, M., Packer, M., & Cardoso, L. (2017). Human cochlear hydrodynamics: A high-resolution μCT-based finite element study. *Journal of Biomechanics*, *50*, 209–216. https://doi.org/10.1016/j.jbiomech.2016.11.020

Hochmair-Desoyer, I. J., Hochmair, E. S., & Burian, K. (1983). Design and fabrication of multiwire scala tympani electrodes. *Annals of the New York Academy of Sciences*, *405*(1), 173–182. https://doi.org/10.1111/j.1749-6632.1983.tb31630.x

Loeb, G. E. (1990). Cochlear prosthetics. *Annual Review of Neuroscience*, *13*(1), 357–371. https://doi.org/10.1146/annurev.ne.13.030190.002041

Loizou, P. C. (1998). Mimicking the human ear. *IEEE Signal Processing Magazine*, *15*(5), 101–130. https://doi.org/10.1109/79.708543

Millar, I. B., Tong, Y. C., & Clark, G. M. (1984). Speech processing for cochlear implant prostheses. *Journal of Speech, Language, and Hearing Research*, *27*(2), 280–296. https://doi.org/10.1044/jshr.2702.280

Parkins, C. W., & Anderson, S. W. (1983). *Cochlear prostheses: An international symposium*. USA: New York Academy of Sciences.

Sands, T. (2019). Comparison and interpretation methods for predictive control of mechanics. *Algorithms*, *12*(11), 232. https://doi.org/10.3390/a12110232

von Békésy, G. (1959). Similarities between hearing and skin sensations. *Psychological Review*, *66*(1), 1–22. https://doi.org/10.1037/h0046967

von Békésy, G. (1963). Hearing theories and complex sounds. *The Journal of the Acoustical Society of America*, *35*(4), 588–601. https://doi.org/10.1121/1.1918543

von Békésy, G. (1970). Travelling waves as frequency analysers in the cochlea. *Nature*, *225*(5239), 1207–1209. https://doi.org/10.1038/2251207a0

Wilson, B. S., & Dorman, M. F. (2012). Signal processing strategies for cochlear implants. In M. J. Ruckenstein (Eds.), *Cochlear implants and other implantable hearing devices* (pp. 31–46). Plural Publishing.

How to Cite: Parmar, P. & Sands, T. (2023). Hearing Aid System Response Improvement. *Journal of Computational and Cognitive Engineering*, 2(4), 304–311, https://doi.org/10.47852/bonviewJCCE3202768

Appendix A. List of Abbreviations

Symbol	Description
e	Error vector for that method
p	Order of denominator in ARMA
q	Order of numerator in ARMA
r	Order of residual terms in ARMA
t	Time (independent variable)
$\boldsymbol{u}$	Vector of inputs
$u(t)$	Input at time t
y	Vector of outputs
$y(t)$	Output at time t
Symbol	Description
J	Cost function
K	Gain vector
P	Inverse of sample covariance
α_i	ARMA coefficients of outputs
β_i	ARMA coefficients of inputs
$\boldsymbol{\Phi}$	Vector of input, output and error (if applicable) history
θ	Vector of ARMA coefficients
$\hat{\theta}$	Estimate of θ

The list of acronyms is provided in Table A1.

Table A1
List of Acronyms

Acronyms	Description
ARMA	Auto Regressive Moving Average
BM	Basilar Membrane
ELS	Extended Least Squares
ELS-PR	Extended Least Squares – Posteriori Residuals
FIR	Finite Impulse Response
LMS	Least Mean Squares
RLS	Recursive Least Squares
RMS	Root Mean Square
PID	Proportional Integrator Derivative Controller
MPC	Model Predictive Controller

Appendix B. Human Auditory System

Functions of each region are also elaborated in this section. Figure B1 differentiates among the regions of ear.

Figure B1
Different regions of Ear: (a) Outer ear, (b) Middle ear, and (c) Inner ear (Image courtesy of ("EarQ" 2022))

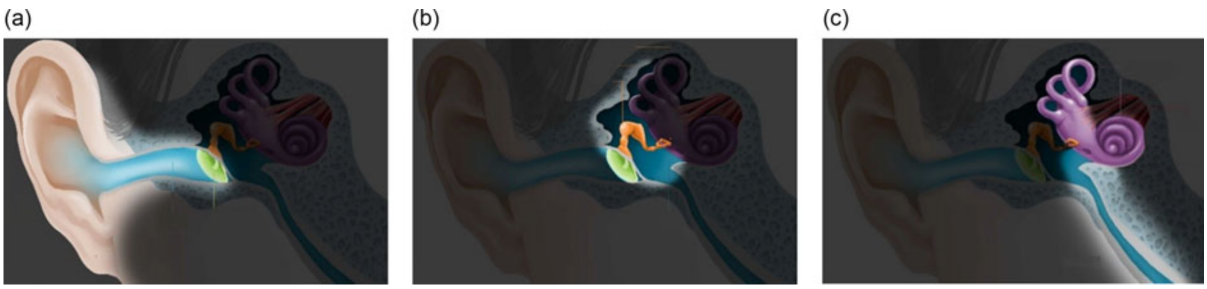

Outer ear

The outer ear (refer Figure B1) consists of auricle, ear canal, and outer layer of eardrum. The auricle collects the acoustic waves from surroundings and directs them to ear canal. The ear canal directs these waves to the outer eardrum. Acoustic waves vibrate the eardrum upon impact.

Middle ear

The middle ear (refer Figure B1) mainly consists of eardrum, bones named ossicles, and oval window. Note that the middle ear consists of lot many other parts which are omitted in this discussion due to their irrelevance. The vibration of eardrums due to acoustic waves is transmitted to ossicles, which are three sets of linked bones. These three bones amplify vibrations of eardrums and transmit them to oval window. The oval window is just a membrane connected to the inner ear.

Inner ear

The inner ear (refer Figure B1) consists of two main functional systems, vestibular system for balancing and head orientation and cochlea for auditory system. The oval window is connected to cochlea. Cochlea (shown in Figure B2) is a snail-shaped spiral organ containing fluid. The vibrations transmitted by oval window to cochlea create surface waves in fluid, actuating hair bundle-like structures in cochlea call stereocilia. The movement of stereocilia is detected by hair cells, which form the base, which translate the movement to neuroelectric signals. Auditory nerve cells (not shown in figures) are connected to hair cells, which carry these neuroelectric signals to the brain.

Figure B2
Visuals of inner ear, (a) demonstration of contact between cochlea and oval window, (b) the waves in ear fluid, stereocilia, and hair cells (Image taken from (Wikipedia, n.d.))

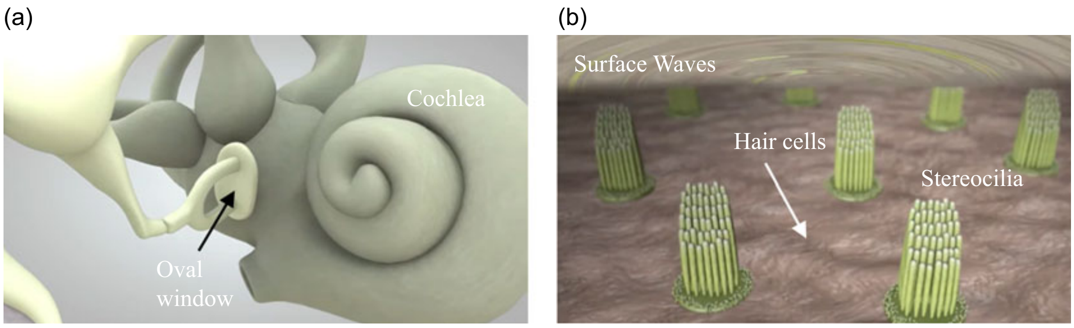

Finally, the brain interprets the neuroelectric signals and perceives different sounds.

Appendix C. Cochlear implant system

As described by Loizou (1998), there are generally two types of stimulations given by electrodes to the auditory nerves,

(i) Analog: Information is present in analog form. In this, electrical analog of acoustic signal is directly transmitted to electrodes. A major disadvantage of this method is that if the stimulation is required to be done simultaneously, the actuation of one electrode will be reflected in output of another, creating unwanted noise.
(ii) Pulsatile: Information is present in terms of pulses. Narrow pulses of information allow all the signals to be sent with different delays, ensuring no interaction of electrodes. The frequency of these pulses determines speech recognition of hearing aid device. It was observed that high pulse rate improves speech recognition but runs at risk of electrode interaction if pulses are too close.

The transmission of the microphone signals to electrodes is done by two methods:

(i) Transcutaneous system: In this system, the signal is transmitted via radio signals across the skin. Main advantage of this method is after insertion of electrodes in patient's inner ear, the skin can be stitched closed which avoids further infection. However, in case of radio reception device failure, the skin will have to be cut open again.
(ii) Percutaneous system: In this system, the signal is directly transmitted to electrodes via plugged connection, reducing circuitry inside the human scalp. Having plug connection on skin can be hazardous and uncomfortable.

Figure C1 shows the difference between two methods of signal transmission.

Figure C1
Schematic representation of transmission methods. (Image courtesy of Loizou (1998))